Article

SOURCE DATA | TRANSPARENT PROCESS | OPEN ACCESS

EMBO reports

The HACE1 E3 ligase mediates RAC1-dependent control of mTOR signaling complexes

Busra Turgu[1,2], Amal El-Naggar[1,3,4], Melanie Kogler[5], Luigi Tortola[5,6], Hai-Feng Zhang[1], Mariam Hassan[1], Michael M Lizardo[1], Sonia HY Kung[7], Wan Lam[1,3], Josef M Penninger[5,8,9,10] & Poul H Sorensen[1,3,*]

Abstract

HACE1 is a HECT family E3 ubiquitin–protein ligase with broad but incompletely understood tumor suppressor activity. Here, we report a previously unrecognized link between HACE1 and signaling complexes containing mammalian target of rapamycin (mTOR). HACE1 blocks mTORC1 and mTORC2 activities by reducing mTOR stability in an E3 ligase-dependent manner. Mechanistically, HACE1 binds to and ubiquitylates Ras-related C3 botulinum toxin substrate 1 (RAC1) when RAC1 is associated with mTOR complexes, including at focal adhesions, leading to proteasomal degradation of RAC1. This in turn decreases the stability of mTOR to reduce mTORC1 and mTORC2 activity. HACE1 deficient cells show enhanced mTORC1/2 activity, which is reversed by chemical or genetic RAC1 inactivation but not in cells expressing the HACE1-insensitive mutant, RAC1^{K147R}. *In vivo*, *Rac1* deletion reverses enhanced mTOR expression in KRas^{G12D}-driven lung tumors of *Hace1*$^{-/-}$ mice. HACE1 co-localizes with mTOR and RAC1, resulting in RAC1-dependent loss of mTOR protein stability. Together, our data demonstrate that HACE1 destabilizes mTOR by targeting RAC1 within mTOR-associated complexes, revealing a unique ubiquitin-dependent process to control the activity of mTOR signaling complexes.

Keywords E3 ubiquitin ligase; HACE1; mTORC1 and mTORC2; RAC1; tumor suppressor gene

Subject Categories Cancer; Post-translational Modifications & Proteolysis; Signal Transduction

DOI 10.15252/embr.202356815 | Received 11 January 2023 | Revised 25 September 2023 | Accepted 29 September 2023 | Published online 17 October 2023

EMBO Reports (2023) 24: e56815

Introduction

HACE1 (HECT domain and ankyrin repeat-containing E3 ubiquitin–protein ligase) was first identified as a tumor suppressor gene in sporadic Wilms' tumor (WT) from analysis of the chromosome 6q21 breakpoint in a t(6; 15)(q21;q21) translocation in a 5-month-old male patient (Fernandez *et al*, 2001; Anglesio *et al*, 2004). HACE1 contains six N-terminal ankyrin repeats, responsible for protein–protein interactions and binding to its ligase targets, linked to a C-terminal HECT domain responsible for its E3 ubiquitin–protein ligase activity (Anglesio *et al*, 2004). *HACE1* inactivation has since been reported in multiple other tumor types, including ovarian carcinoma, non-Hodgkin's lymphoma, lung carcinoma, pancreatic carcinoma, prostate carcinoma, natural killer (NK) cell malignancies, breast cancer or colorectal cancer (Anglesio *et al*, 2004; Zhang *et al*, 2007; Hibi *et al*, 2008; Stewenius *et al*, 2008; Thelander *et al*, 2008; Sakata *et al*, 2009; Huang *et al*, 2010; Slade *et al*, 2010). Consistent with this, genetic inactivation of *Hace1* in mice leads to the development of multiple late-onset tumors, including sarcomas, breast, lung, and other carcinomas, and lymphomas (Zhang *et al*, 2007). More recently, we showed that HACE1 also displays tumor suppressor activity in osteosarcoma, as HACE1 expression is reduced in this disease and overexpression blocks osteosarcoma xenograft growth and metastasis (El-Naggar *et al*, 2019). Furthermore, we recently reported that under hypoxia, HACE1 regulates the key metastasis driver, hypoxia-inducible factor-1alpha (HIF1α), in an E3 ligase-dependent manner (Turgu *et al*, 2021). However, the full spectrum by which HACE1 exerts its tumor suppressive activity remains to be fully elucidated.

In this study, we identified a previously unknown link between HACE1 and signaling complexes containing mammalian targets of

1 Department of Molecular Oncology, British Columbia Cancer Research Centre, Vancouver, BC, Canada
2 Faculty of Medicine, University of British Columbia, Vancouver, BC, Canada
3 Department of Pathology and Laboratory Medicine, University of British Columbia, Vancouver, BC, Canada
4 Department of Pathology, Faculty of Medicine, Menoufia University, Shibin El Kom, Egypt
5 Institute of Molecular Biotechnology of the Austrian Academy of Sciences, Vienna, Austria
6 Department of Biology, Institute of Molecular Health Sciences, ETH Zurich, Zurich, Switzerland
7 Department of Urological Sciences, Vancouver Prostate Centre, University of British Columbia, Vancouver, BC, Canada
8 Department of Medical Genetics, Life Sciences Institute, University of British Columbia, Vancouver, BC, Canada
9 Department of Laboratory Medicine, Medical University of Vienna, Vienna, Austria
10 Helmholtz Centre for Infection Research, Braunschweig, Germany
*Corresponding author. Tel: +1 (604) 675 8202; Fax: +1 (604) 675 8218; E-mail: psor@mail.ubc.ca

rapamycin, mTOR, uncovering a new ubiquitin-dependent molecular mechanism to control mTOR-associated complexes. The mTOR protein is a component of two structurally and functionally distinct complexes, namely, mTOR complex 1 (mTORC1) and mTOR complex 2 (mTORC2). The mTORC1 is a major regulator of growth and nutrient responses in mammalian cells and has well-established roles in cancer pathogenesis (Mossmann *et al*, 2018; Murugan, 2019). This complex is defined by its three core components: mTOR, RAPTOR (regulatory protein associated with mTOR), and mLST8 (mammalian lethal with Sec13 protein 8, also known as GβL; Kim *et al*, 2002; Saxton & Sabatini, 2017). The kinase activity of mTORC1 directly phosphorylates the translational regulators eukaryotic translation initiation factor 4E (eIF4E) binding protein 1 (4E-BP1) and S6 kinase 1 (S6K1), leading to phosphorylation of ribosomal protein S6 (RPS6) and translational activation of a subset of cellular mRNAs (Laplante & Sabatini, 2012; Saxton & Sabatini, 2017). The mTORC2 contains mTOR, rapamycin-insensitive companion of mTOR (RICTOR) and mLST8, and a main downstream substrate of mTORC2 is Akt, a key effector of insulin/PI3K signaling, which is phosphorylated at Ser-473 by mTORC2 in response to diverse stimuli (Saxton & Sabatini, 2017; He *et al*, 2021). Despite the critical roles of mTORC1 and mTORC2 in both normal cell physiology and cancer biology, how their activities are controlled by ubiquitin-dependent molecular mechanisms remains incompletely understood.

We report that HACE1 inhibits both mTORC1 and mTORC2 activity in an E3 ligase-dependent manner. Inhibition requires HACE1-mediated ubiquitylation and degradation of the RAC1 (Ras-related C3 botulinum toxin substrate 1) GTPase, previously identified as an E3 ligase substrate of HACE1 (Torrino *et al*, 2011; Mettouchi & Lemichez, 2012; Castillo-Lluva *et al*, 2013; Daugaard *et al*, 2013; Goka & Lippman, 2015; Acosta *et al*, 2018). RAC1 belongs to the family of small GTPases (20–25 kDa) which cycle between their GDP-bound inactive state and a GTP-bound active state (Day *et al*, 1998; Gao *et al*, 2004). Upon activation, small GTPases interact with their effector proteins leading to induction of downstream signaling pathways (Day *et al*, 1998; Duran & Hall, 2012; Cardama *et al*, 2017). Recently, we showed that in Hace1 deficient mice with $KRas^{G12D}$-driven lung tumors, concomitant inactivation of Rac1 blocks lung tumorigenesis and progression (Kogler *et al*, 2020). RAC1 was previously reported to positively regulate both mTORC1 and mTORC2 signaling through direct interactions with these complexes (Saci *et al*, 2011; Hervieu *et al*, 2020). We show that *in vivo*, $Hace1^{-/-}$ mice exhibit increased mTOR protein expression, and genetic deletion of *Rac1* in $Hace1^{-/-}$ mice reversed the observed increase in mTOR expression, providing direct genetic evidence on the epistasis of these pathways *in vivo*. Together, our data provide new mechanistic insights into the tumor suppressor activity of HACE1 through the regulation of mTORC1 and mTORC2 signaling, and, furthermore, reveal a ubiquitin-dependent molecular mechanism that controls the activity of mTOR signaling complexes.

Results

HACE1 negatively regulates mTOR signaling complexes

To assess links between HACE1 and mTOR signaling, we first used Western blotting to assess established readouts of mTORC1 signaling, namely, p-S6K1, p-S6, p-4EBP1, and for mTORC2, namely p-Ser473-AKT, in HEK293 cells stably expressing HACE1 versus control cells containing empty vector alone. HACE1 overexpression reduced mTORC1 and mTORC2 activity compared to controls, not only under ambient conditions but also under serum starvation, 1% hypoxia, and EGF treatment, a known physiological stimulus of both mTORC1 and mTORC2 activity (Galbaugh *et al*, 2006; Morrison Joly *et al*, 2017; Fig 1A). To validate these findings in a second cell system, we measured the same readouts in wild type (*wt*) versus $Hace1^{-/-}$ mouse embryonic fibroblasts (MEFs). Accordingly, $Hace1^{-/-}$ cells showed an increase in mTORC1 and mTORC2 activity compared to *wt* cells (Fig 1B) which was reversed by *HACE1* re-expression in $Hace1^{-/-}$ MEFs (Fig 1C). Next, we performed stable knockdown (kd) of endogenous HACE1 in HEK293 cells using two independent shRNAs and similarly assessed p-S6K1, p-S6, p-4EBP1, and p-Ser473-AKT levels by Western blotting. HACE1 kd increased readouts of both mTORC1 and mTORC2 activity (Fig 1D), which was supported by immunofluorescence using antibodies to p-mTOR (Appendix Fig S1A and B). Quantification of immunoblots (phospho- versus total proteins) are provided in Appendix Fig S1 (panels C–I). Focusing on mTORC1, we next investigated whether HACE1 decreases mTORC1 activity *in vivo*, we analyzed formalin-fixed paraffin-embedded (FFPE) tissues from nude mice bearing xenografted HEK293 tumors with or without stable *HACE1* kd as described (Zhang *et al*, 2007), using immunohistochemistry (IHC) for p-S6 and p-4EBP1 expression as downstream mTORC1 readouts. In agreement with our *in vitro* observations, *HACE1* kd led to increased mTORC1 activity *in vivo* (Fig 1E; quantified in F–H). In addition, we performed histopathological analysis of tumor sections, which revealed sheets of tumor cells exhibiting pleomorphism, increased nucleocytoplasmic ratios, mitotic activity, and extensive areas of necrosis. Tumors with HACE1 inactivation were significantly larger and demonstrated increased mitotic activity and necrotic areas, supporting the tumor suppressor activity of HACE1 (Fig EV1A and B). Together, these data identify previously unrecognized role for HACE1 in regulating mTOR expression levels and mTOR signaling.

HACE1 regulates mTOR signaling in an E3 ligase-dependent manner

To determine if HACE1 requires its E3 ligase activity to regulate mTORC1 and mTORC2 signaling, we first ectopically expressed a previously described ligase dead HACE1-C876S mutant (Zhang *et al*, 2007) in SKNEP1 Ewing sarcoma cells (Fig 2A), which lack endogenous HACE1 expression (Anglesio *et al*, 2004; Zhang *et al*, 2007). While HACE1 overexpression strongly reduced activity of both complexes in these cells, HACE1-C876S failed to do so, particularly in the presence of EGF to stimulate mTOR activity (Fig 2B). Quantification of immunoblots (phospho- versus total proteins) is provided in Appendix Fig S2. Wild type HACE1 overexpression also reduced p-mTOR, p-RPS6, p-S6K, and p-4EBP1 levels as well as p-Ser473-AKT in HEK293 cells, while HACE1-C876S was unable to do so (Fig 2C). The mTORC1 targets remained sensitive to Rapamycin treatment, which still effectively blocked each readout of mTOR activity in HEK293 cells expressing vector alone, HACE1 or ligase dead HACE1 (Fig 2C). Together, these findings demonstrate that the observed effects of HACE1 on mTOR signaling are dependent on HACE1's E3 ligase activity.

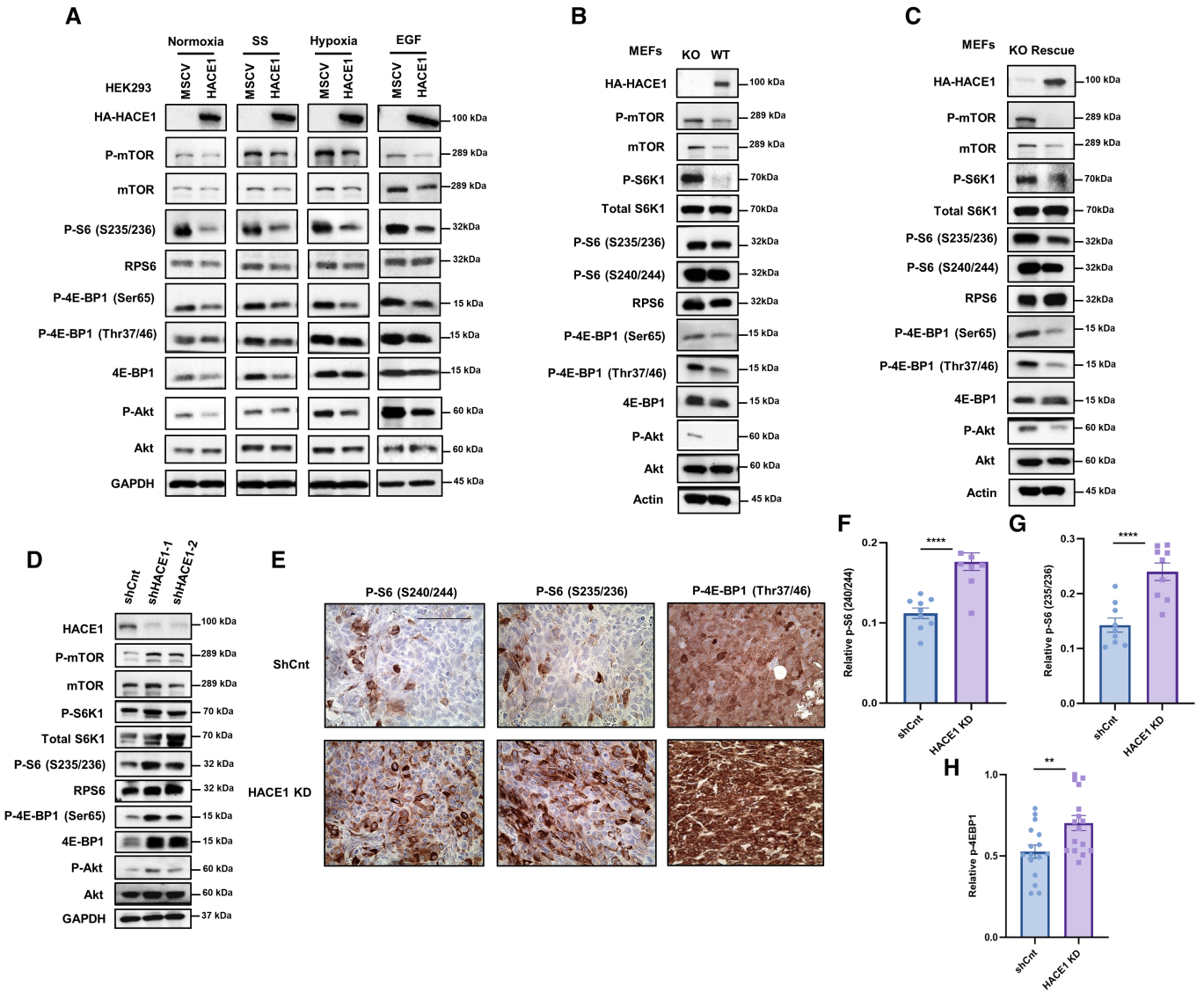

Figure 1. HACE1 regulates mTOR signaling.

A HEK293 cells stably expressing HACE1 and the empty vector alone were grown in 10% serum (Normoxia), subjected to 6 h of serum starvation (SS), exposed to 1% O_2 for 3 h (Hypoxia) and stimulated with 10 ng/ml EGF for 10 min. Protein levels of mTOR signaling downstream targets under these conditions were analyzed by Western blotting.

B Protein levels of mTOR signaling downstream targets were analyzed by Western blotting in Hace1$^{-/-}$ and wild-type MEFs. Actin was used as a loading control.

C HA-tagged HACE1 was re-expressed in Hace1$^{-/-}$ MEFs. Protein levels of mTORC1 downstream targets were analyzed by Western blotting.

D Stable knockdown of HACE1 using two independent shRNAs in HEK293 cells. Protein levels of mTOR signaling downstream targets were analyzed by Western blotting.

E Immunohistochemistry for mTORC1 downstream targets (Phospho-S6 (S240/244), Phospho-S6 (S235/236), and Phospho-4E-BP1 (Thr37/46)) conducted on the paraffin blocks from nude mice injected with HEK293 cells with stable HACE1 knockdown or non-targeting shRNA, generated as described previously (1). (n = 3 mice per group, biological replicates). Scale bar is 100 μm.

F Quantification of Phospho-S6 (S240/244) in (E) was conducted respectively using ImageJ software and data represented as average value ± SEM (n = 3 mice per group, biological replicates). For each group (n = 9) HPFs were analyzed. Data are shown as mean ± SEM, paired t-test comparison test (****P < 0.0001).

G, H Quantification of Phospho-S6 (S235/236) in (E) was conducted respectively using ImageJ software and data represented as average value ± SEM (n = 3 mice per group, biological replicates). For each group (n = 9) HPFs were analyzed. Data are shown as mean ± SEM, paired t-test comparison test (****P < 0.0001) (H) Quantification of Phospho-4E-BP1 (Thr37/46) in (E) was conducted respectively using ImageJ software and data represented as average value ± SEM (n = 3 mice per group). For each group (n = 16) HPFs were analyzed. Data are shown as mean ± SEM, paired t-test comparison test (**P < 0.01).

Source data are available online for this figure.

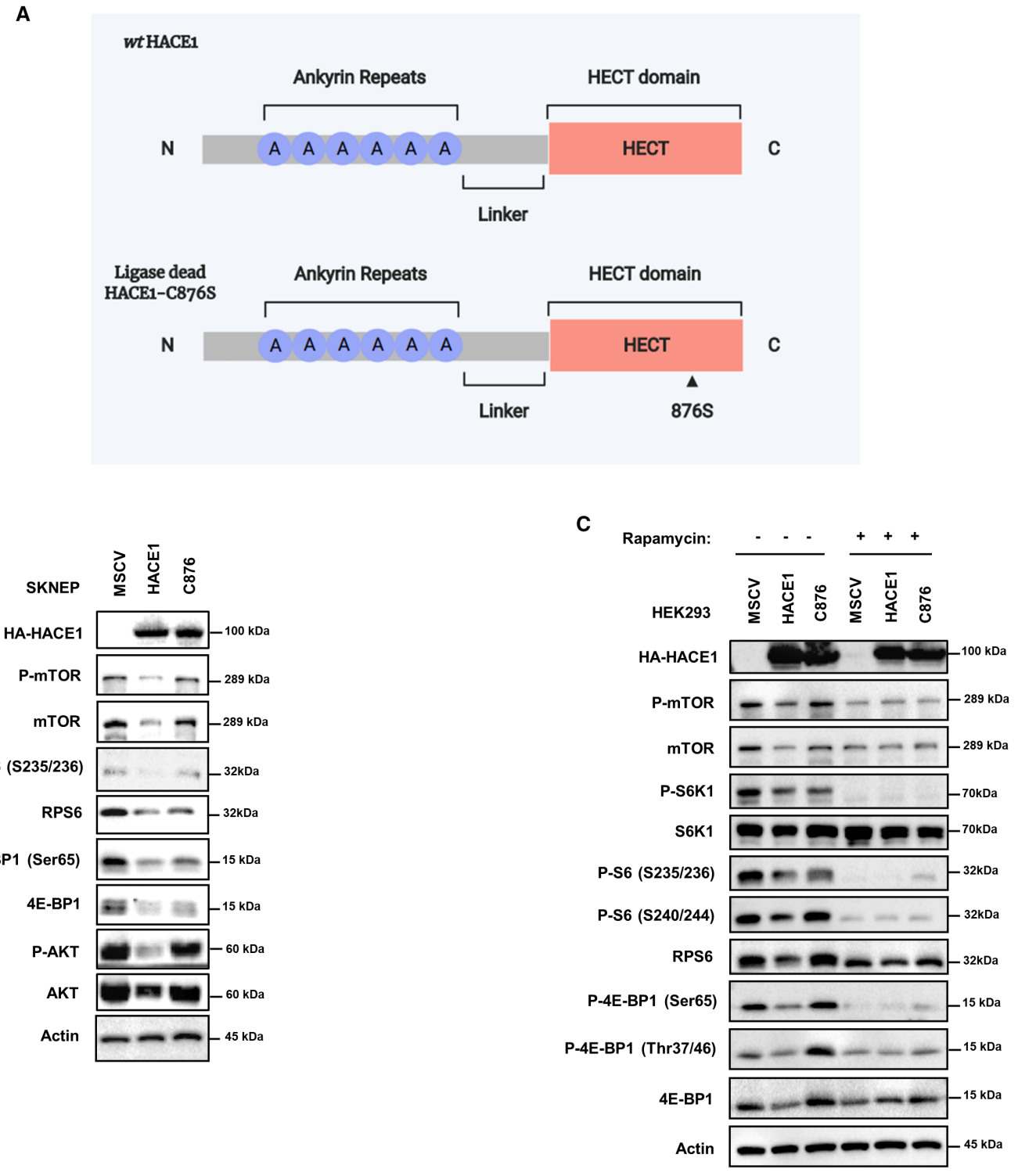

Figure 2. Effect of HACE1 on mTORC1 signaling is dependent on its E3 ligase activity.

A A diagram showing the structures of wild type (wt) and the ligase dead mutant HACE1 C876S proteins.

B SKNEP cells expressing HA-HACE1, ligase dead HACE1-C876S and empty vector alone were grown in 10% serum and pulsed with 10 ng/ml EGF for 15 min. Protein levels of mTORC1 downstream targets were analyzed by Western blotting.

C HEK293 cells stably expressing HACE1, ligase dead HACE1-C876S and the empty vector alone were treated or not with 10 nM Rapamycin for 1 h. Protein levels of mTORC1 downstream targets were analyzed by Western blotting.

Source data are available online for this figure.

Loss of HACE1 enhances mTOR protein stability

Unexpectedly, our data showed that total mTOR protein levels were markedly reduced in HACE1 proficient cells (Figs 1A–C and 2C). We therefore tested whether HACE1, a known E3 ligase, might target mTOR or its complex component through ubiquitin-mediated proteasomal degradation. Indeed, in cycloheximide chase experiments, we found that mTOR itself is much more stable in control HEK293 cells expressing vector alone compared to those stably expressing HACE1 (Fig 3A; quantified in B). To expand this finding to a different cell system, we next compared mTOR stability in *Hace1*$^{-/-}$ versus *wt* MEFs. HACE1 KO MEFs showed markedly increased mTOR stability (Fig 3C; quantified in D), and *HACE1* re-expression markedly decreased mTOR stability in these cells (Fig 3E; quantified in F). However, expression of ligase dead HACE1-C876S failed to alter mTOR stability in the same cells (Fig 3G; quantified in H). Corresponding expression of HACE1 in each cell type is shown in Fig 3I and J). To assess whether proteasome activity is required for HACE1-mediated effects on mTOR stability, HEK293 and *Hace1*$^{-/-}$ MEFs cells stably expressing HACE1 or vector alone were treated with the proteasome inhibitor MG132 for 2 h. MG132 completely blocked the ability of HACE1 to reduce mTOR levels in either cell type (Fig 3K and L). To rule out the possibility of transcriptional regulation of mTORC1 signaling by HACE1, we compared mRNAs encoding mTOR and several key mTORC1 targets (4EBP1 and RPS6) in HEK293 cells stably expressing HACE1 versus empty vector but failed to observe differential expression of these transcripts (Fig EV2), arguing against transcriptional regulation by HACE1. Together, these results indicate that HACE1 reduces stability of mTOR protein in an E3 ligase-dependent manner.

HACE1 inhibits mTOR signaling by targeting RAC1

We next explored whether HACE1 directly ubiquitylates mTOR using established *in vitro* ubiquitylation assays but found no evidence for such an activity (see Fig EV3A), indicating that the process may be indirect. To date, the best characterized and established E3 ligase target of HACE1 is the active form of RAC1, as HACE1 binds and targets active as opposed to total RAC1 for ubiquitylation and proteasomal degradation (Torrino *et al*, 2011; Mettouchi & Lemichez, 2012; Castillo-Lluva *et al*, 2013; Daugaard *et al*, 2013; Goka & Lippman, 2015; Acosta *et al*, 2018). Since RAC1 is reported to regulate both mTORC1 and mTORC2 (Saci *et al*, 2011; Hervieu *et al*, 2020), we wondered whether HACE1 regulates mTOR signaling through RAC1. We first incubated HEK293 cells stably expressing empty vector or *wt* HACE1 with EHT1864, a selective inhibitor of RAC1 activation which traps RAC1 in an inactive state (Shutes *et al*, 2007), thereby inhibiting RAC1 downstream signaling and RAC1-mediated functions *in vivo* (Onesto *et al*, 2008). Active and total RAC1 levels were measured using a commercial RAC1 activation kit (see Materials and Methods) in cells treated with or without EHT1864 treatment. EHT1864 effectively prevented RAC1 activation in both control and HACE1 overexpressing cells (Fig 4A). In addition, EHT1864 also blocked downstream targets of activated mTOR signaling including p-mTOR, p-RPS6, p-S6K, and p-4EBP1, as well as p-Ser473-AKT (Fig 4B), similar to what we observed above for known mTOR inhibitors, Rapamycin (Fig 2C) and Torin1 (Fig EV3B), confirming that RAC1 regulates mTOR signaling.

Next, we inactivated RAC1 with two independent shRNAs in HEK293 cells to directly test whether RAC1 kd affects mTOR signaling (Fig 4C). Indeed, RAC1 kd markedly reduced mTORC1 and mTORC2 activation in HACE1 deficient cells, which was completely rescued by re-expressing siRNA resistant RAC1 in the same cells (Fig 4C). Moreover, overexpression of RAC1 itself markedly enhanced mTORC1 activity (Fig 4D). Finally, to further validate the link to HACE1, we used a RAC1-K147R mutant that is resistant to HACE1 degradation, due to substitution of the RAC1 lysine K147 residue targeted for HACE1-mediated ubiquitylation (Torrino *et al*, 2011; Mettouchi & Lemichez, 2012; Castillo-Lluva *et al*, 2013; Daugaard *et al*, 2013; Goka & Lippman, 2015; Acosta *et al*, 2018). In HEK293 cells stably co-expressing ectopic HACE1 along with vector alone, *wt* RAC1, or RAC1-K147R, HACE1 blocked mTORC1 signaling and p-Ser473-AKT in control and *wt* RAC1 expressing cells (Fig 4E; lanes 2 and 4) but had no apparent effect in cells expressing HACE1-resistant RAC1-K147R (Fig 4E; lanes 5 and 6). These findings provide direct evidence that HACE1 regulates mTOR signaling through RAC1 and confirm that active RAC1 is a positive regulator of mTORC1 and mTORC2 signaling in these cells.

HACE1 targets RAC1 when it is associated with mTOR complexes

As RAC1 has been reported to be a component of both mTORC1 and mTORC2 complexes (Duran & Hall, 2012; Xie & Proud, 2014), we hypothesized that HACE1 might target RAC1 for proteasomal degradation when it is bound to these complexes. Focusing on mTORC1, we first tested whether HACE1 physically associates with mTORC1. Using an HA pull-down assay, we observed that mTOR, RAPTOR and RAC1 could each be co-immunoprecipitated (co IP'ed) with HA-HACE1 in HEK293 cells (Fig 5A and B). Notably, these interactions were dramatically inhibited by RAC1 kd (Fig 5B), suggesting that HACE1 targets RAC1 when the latter is associated with mTORC1. To validate this finding, we analyzed whether mTOR is required for RAC1 ubiquitylation by HACE1 as assessed by GST-Tube pulldown assays. Accordingly, mTOR kd using two independent siRNAs blocked HACE1-mediated ubiquitylation of RAC1 (Fig 5C). Moreover, HACE1 overexpression increased the levels of ubiquitylated RAC1, mTOR and RAPTOR proteins (Fig 5C). To further probe how mTOR complex formation affects ubiquitylation of RAC1 in the presence of HACE1, we knocked down either RAPTOR or RICTOR using independent siRNAs targeting each protein to reduce complex formation. Inactivation of either RAPTOR or RICTOR reduced HACE1-mediated ubiquitylation of RAC1 (Fig EV4A), suggesting that RAC1 ubiquitylation by HACE1 occurs in mTOR complexes. To verify this finding, we assessed mTOR-associated ubiquitinated proteins in HEK293 cells with HACE1 kd (Fig 5D) or overexpression (Fig 5E). IP's using anti-mTOR antibodies pulled down elevated amounts of ubiquitylated mTOR-associated proteins in *HACE1* overexpressing cells compared to controls (Fig 5D), while HACE1 inactivation noticeably decreased ubiquitylated proteins compared to shCnt cells (Fig 5E). Next, to show specific ubiquitylation within these complexes, we transfected cells with GFP-ubiquitin followed by anti-GFP IP's to pull down ubiquitylated proteins. We observed that HACE1 knockdown decreases levels of ubiquitylated mTOR and RAC1 (Fig 5F), while overexpression increases their specific ubiquitylation in ubiquitin-containing complexes (Fig 5G). While not ruling out RAC1 is also targeted by HACE1 within other molecular

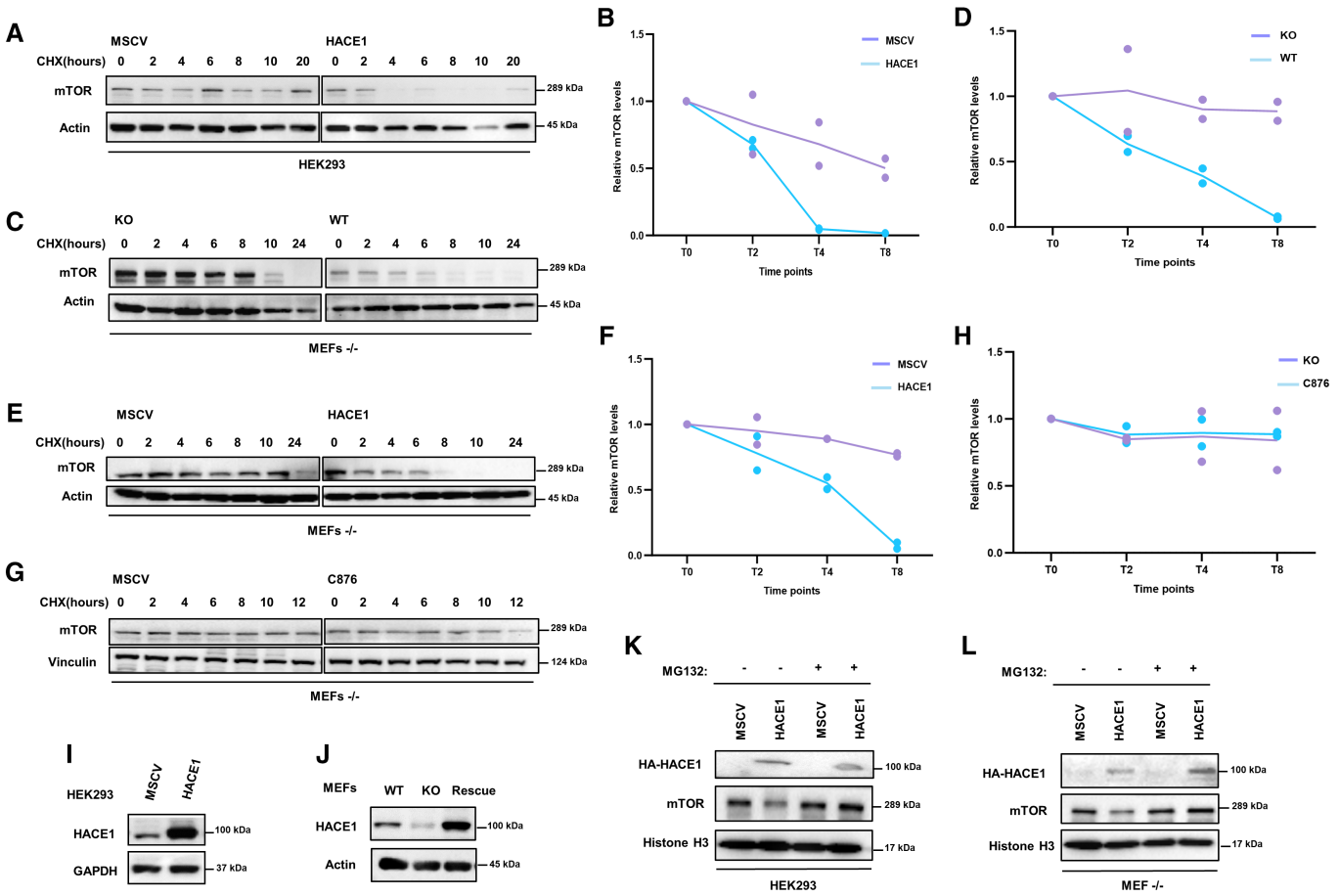

Figure 3. HACE1 decreases mTOR protein stability.

A HEK293 cells stably overexpressing HACE1 or vector alone were treated with cycloheximide (CHX) for the indicated time points to block protein synthesis, and lysates were analyzed for mTOR levels by Western blotting.

B Graph showing quantified mTOR protein amounts normalized to actin levels in (A) (n = 2 technical replicates). Data were replicated three times.

C Hace1$^{-/-}$ MEFs and wt MEF cells were treated with CHX for the indicated time points, and lysates were analyzed for mTOR levels by Western blotting.

D Graph showing quantified mTOR protein amounts normalized to actin levels in (C) (n = 2 technical replicates). Data were replicated three times.

E Hace1$^{-/-}$ MEFs stably expressing HA-HACE1 was treated with CHX for the indicated time points, and lysates were analyzed for mTOR levels by Western blotting.

F Graph showing quantified mTOR protein amounts normalized to actin levels in (E) (n = 2 technical replicates). Data were replicated three times.

G Hace1$^{-/-}$ MEFs stably expressing C876-HACE1 was treated with CHX for the indicated time points, and lysates were analyzed for mTOR levels by Western blotting.

H The graph shows quantified mTOR protein amounts normalized to actin levels in (G) (n = 2 technical replicates). Data were replicated three times.

I Whole protein lysates were collected to examine the levels of HACE1 protein in HEK293 cells stably expressing HACE1 and empty vector alone (MSCV). Protein levels of HACE1 were analyzed by Western blotting.

J Whole protein lysates were collected to examine the levels of HACE1 protein in Hace1$^{-/-}$ MEF cells, Hace1 wt cells and Hace1$^{-/-}$ MEF cells stably expressing HACE1. Protein levels of HACE1 were analyzed by Western blotting.

K, L HEK293 cells and Hace1$^{-/-}$ MEFs stably overexpressing HACE1 or vector alone were treated with the proteasome inhibitor MG132 for 2-h, and lysates were analyzed for mTOR levels by Western blotting.

Source data are available online for this figure.

complexes, these data indicate that HACE1 ubiquitylation of RAC1 occurs when the latter is a component of mTOR signaling complexes, which is associated with increased ubiquitylation of mTOR itself.

Next, we wished to determine where in the cell HACE1 might target mTOR complexes. Using HEK293 cells expressing HA-HACE1, we observed that HACE1 and mTOR colocalize predominantly in perinuclear punctate structures, potentially located near the cell periphery (Fig 5H). Since it has recently been shown that mTOR can associate with focal adhesions (Rabanal-Ruiz *et al*, 2021) and HACE1 is known to localize to plasma membranes (Daugaard *et al*, 2013), we speculated that HACE1 and mTOR might interact at focal adhesions. We therefore used two well established markers of focal adhesion formation, Paxillin and FAK (Hu *et al*, 2014). In HEK293 cells expressing HA-HACE1 both Paxillin and FAK colocalized with HACE1 (Fig 5I) and mTOR (Fig 5J). We then used Pearson's coefficient analysis to assess overlaps between GFP-FAK and Paxillin with HACE1 and mTOR, as quantified in Fig EV4B and C, respectively. Intensity profiles of the high magnification images from Fig 5I and J was then performed, showing robust overlap of

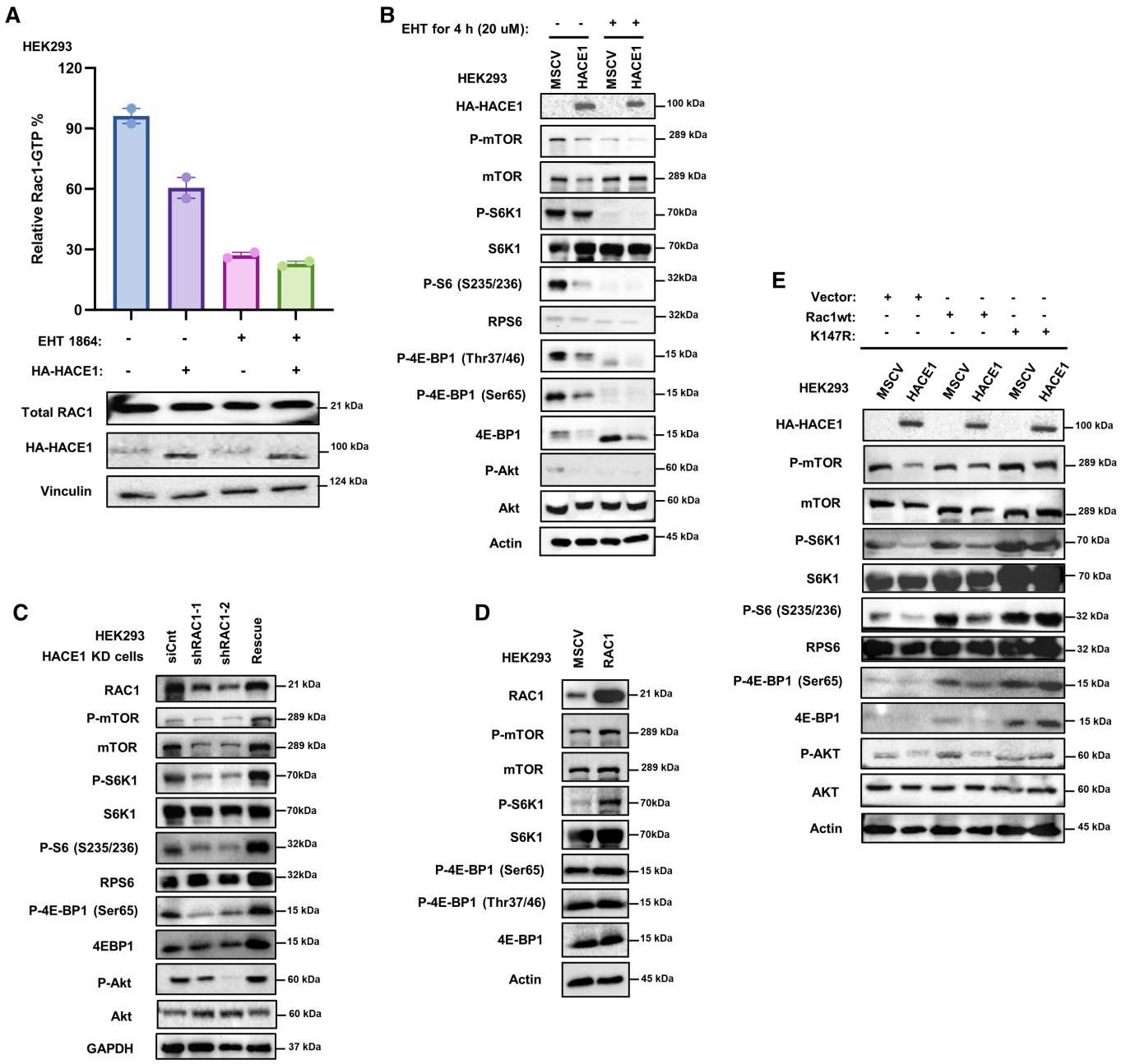

Figure 4. HACE1 decrease mTORC1 signaling through RAC1.

A GTP bound RAC1 levels are shown using RAC1 G-LISA Activation Assay Kit in the cells stably expressing HACE1 or the empty vector controls in the presence or absence of EHT 1864. Total RAC1 levels are shown by Western blotting (n = 2 technical replicates). Data were replicated three times.

B HEK293 cells stably expressing HACE1 or the empty vector alone were treated (or not treated) with 20 μM EHT 1864 for 1-h. Protein levels of mTORC1 downstream targets were analyzed by Western blotting.

C HEK293 cells with stable HACE1 KD were transfected with control shRNA (Scr) or one of two independent shRNAs targeting RAC1 (shRAC1). Rescue is generated by re-introducing pHAGE-RAC1 plasmid to the cells using a lentiviral transduction system. Protein levels of mTORC1 downstream targets were analyzed by Western blotting.

D HEK293 cells were transfected with pHAGE-RAC1 plasmid using a lentiviral transduction system, then subjected to western blotting for the analysis of mTORC1 downstream targets.

E HEK293 cells stably expressing HACE1 or the empty vector alone were transfected with combinations of wild-type RAC1, RAC1-K147R and vector alone, then subjected to western blotting for the analysis of mTORC1 downstream targets.

Source data are available online for this figure.

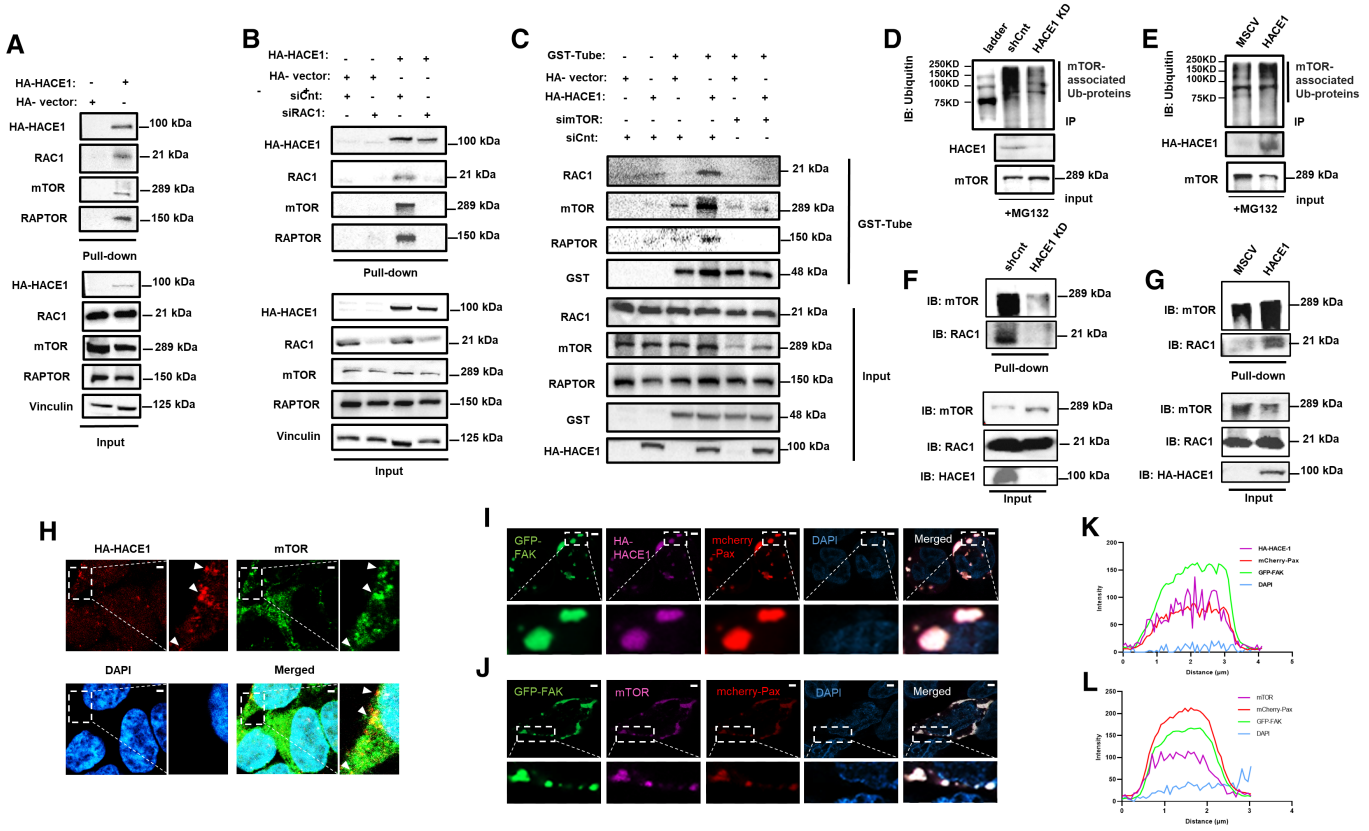

Figure 5. HACE1 targets RAC1 when RAC1 is bound to mTORC1.

A HEK293 cells stably expressing HA-HACE1 or the empty vector alone were incubated with 10 μM MG132, before being subjected to HA pull downs of HACE1 interacting molecules and analyzed by immunoblotting for the indicated proteins.

B HEK293 cells stably expressing HA-HACE1 or the empty vector alone transfected with siRNA control (siCnt) or siRNA Rac1 (siRAC1) as indicated for 72 h, were subjected to HA pull-downs of HACE1 interacting molecules and analyzed by immunoblotting for the indicated proteins.

C HEK293 cells stably expressing HA-HACE1 or the empty vector alone transfected with siRNA control (siCnt) or siRNA mTOR (simTOR) siRNAs for 72 h, were incubated with 10 μM MG132 and lysed with or without GST-TUBE2 as indicated, before being subjected to GST pull-downs and analyzed by immunoblotting for the indicated ubiquitylated proteins.

D HEK293 cells with stable HACE1 knockdown or non-targeting shRNA were incubated with 10 μM MG132, before being subjected to pull downs using mTOR antibody and analyzed by immunoblotting for the indicated proteins.

E HEK293 cells stably expressing HA-HACE1 or the empty vector alone were incubated with 10 μM MG132, before being subjected to pull downs using mTOR antibody and analyzed by immunoblotting for the indicated proteins.

F HEK293 cells with stable HACE1 knockdown or non-targeting shRNA transfected with GFP-ubiquitin plasmid for 48 h, were incubated with 10 μM MG132 for 2 h before being subjected to pull downs using GFP antibody and analyzed by immunoblotting for the indicated proteins.

G HEK293 cells stably expressing HA-HACE1 or the empty vector alone transfected with GFP-ubiquitin plasmid for 48 h, were incubated with 10 μM MG132 for 2 h before being subjected to pull downs using GFP antibody and analyzed by immunoblotting for the indicated proteins.

H HA-HACE1 expressing HEK293 cells were immunostained for HA and mTOR and analyzed by immunofluorescence. Arrowheads indicate the areas of co-localization of mTOR and HACE1. Scale bar is 50 μm.

I HA-HACE1 expressing HEK293 cells were transfected with GFP-FAK and mCherry-Paxillin (as a positive control) plasmids. After 48 h, cells were seeded on fibronectin pre-coated chambers and immunostained with HA or mTOR primary antibodies directly conjugated to Alexa 647; dilution 1:100) overnight at 4°C. Next day, wells were washed with PBS with 0.05% triton-X twice for 5 min. Chambers were carefully removed and mounted with Vectashield with DAPI (Vectorlabs). Slides were imaged using 63× objective of a Zeiss LSM 800 Airyscan confocal microscope (n = 3 biological replicates) (blue: DAPI; red: mCherry-Paxillin; green: GFP-FAK; pink: HA-HACE1). Scale bar is 5 μm.

J HA-HACE1 expressing HEK293 cells were transfected with GFP-FAK and mCherry-Paxillin plasmids. After 48 h, cells were seeded on fibronectin coated chambers and immunostained with mTOR antibody directly conjugated with Alexa-647. (n = 3 biological replicates) (blue: DAPI; red: mCherry-Paxillin; green: GFP-FAK; pink: mTOR). Scale bar is 5 μm.

K The intensity profile of (I) shows overlap of the green, red and pink signals in the same areas (n = 3 biological replicates).

L The intensity profile of (J) shows overlap of the green, red and pink signals in the same areas (n = 3 biological replicates).

Source data are available online for this figure.

either HACE1 (Fig 5K) or mTOR (Fig 5L) with Paxillin and FAK, providing further evidence for co-localization of mTOR and HACE1 in focal adhesions. Finally, we performed 3-dimensional (3D) imaging, as shown in videos with Z-stack images for each channel in Fig EV4D, and Movies EV1 and EV2, respectively. Again, these data show colocalization of HACE1, mTOR, Paxillin, and FAK. However,

these findings do not rule out that HACE1 targets RAC1 at mTORC1 complexes located at other cellular structures containing Paxillin and FAK.

Reduced HACE1 expression correlates with increased mTOR levels *in vivo*

To confirm the link between HACE1 and mTOR regulation *in vivo*, we next performed IHC to assess mTOR expression in formalin-fixed paraffin-embedded (FFPE) tissues from nude mice with SKNEP1 xenograft tumors. The latter were generated by flank injection of SKNEP1 cells stably expressing either *wt* HACE1, HACE1-C876S, or vector alone, as previously described (Zhang *et al*, 2007). In agreement with our *in vitro* observations, tumors expressing wild-type HACE1 showed decreased levels of mTOR expression compared to tumors from cells stably expressing vector alone or ligase dead HACE1 (Fig 6A; quantified in B), indicating that HACE1 reduces mTOR expression *in vivo* in an E3 ligase-dependent manner. Previously, Kogler *et al* (2020) reported that 41 of 292 known *HACE1* mutations identified in public databanks occurred in lung cancer patients (lung adenocarcinomas, lung squamous cell carcinomas and small-cell carcinomas). In addition, we previously showed that aged $Hace1^{-/-}$ mice develop spontaneous lung tumors, the rates of which are significantly increased upon urethane treatment, compared to $Hace1^{+/+}$ or $Hace1^{+/-}$ littermate controls (Zhang *et al*, 2007). Based on these findings, and to further investigate the pathophysiological significance of a HACE1/mTORC1 link, we used IHC to assess HACE1 and mTOR protein expression in non-small cell lung cancer (NSCLC) tumor tissues ($n = 5$). Consistent with our previously published results in NSCLC (Turgu *et al*, 2021), endogenous HACE1 protein expression was barely detectable in each tumor case ($n = 5$), in contrast to mTOR which was strongly expressed (Fig 6C and D). To further assess this link in lung tumors, tissue microarrays (TMAs) consisting of SCLC (small cell lung cancer; 50 cases) were assessed by IHC for HACE1 and mTOR expression. A highly significant correlation was observed between strong mTOR and low HACE1 expression in these tumors (Fig 6E and F), highlighting the inverse relationship between HACE1 and mTOR levels in SCLC tumors *in vivo*.

Rac1 deletion reverses enhanced mTOR expression in lung tumors of $Hace1^{-/-}$ mice

To genetically validate these findings *in vivo*, we used a mouse lung cancer model of *Hace1* inactivation in which deletion of *Rac1* and expression of oncogenic $KRas^{G12D}$ is simultaneously induced by Adeno-Cre administration (Zhang *et al*, 2007; Kogler *et al*, 2020). IHC was performed to assess mTOR expression in FFPE lung tumor tissues obtained from 8- and 16-week-old $KRas^{G12D}Hace1^{+/+}Rac1^{+/+}$, $KRas^{G12D}Hace1^{-/-}Rac1^{+/+}$, $KRas^{G12D}Hace1^{+/+}Rac1^{fl/fl}$, and $KRas^{G12D}Hace1^{-/-}Rac1^{fl/fl}$ mice. In support of the above observations, genetic deletion of *Hace1* alone (i.e. lung tumors in $KRas^{G12D}Hace1^{-/-}Rac1^{+/+}$ mice) resulted in elevated mTOR levels compared to $KRas^{G12D}Hace1^{+/+}Rac1^{+/+}$ control tumors, while genetic inactivation of *Rac1* alone (i.e. $KRas^{G12D}Hace1^{+/+}Rac1^{fl/fl}$ tumors was strongly associated with decreased mTOR levels compared to control tumors (Fig 7A–C). $KRas^{G12D}Hace1^{-/-}Rac1^{fl/fl}$ mouse tumors showed a significant reduction in mTOR levels compared to tumors in $KRas^{G12D}Hace1^{-/-}Rac1^{+/+}$ mice at both 8- and 16-weeks post-induction, indicating that *Rac1* deletion reversed the enhanced mTOR expression observed in lung tumors of $Hace1^{-/-}$ mice (Fig 7A–C). Together, these data strongly support the notion that HACE1 regulates mTOR levels and mTORC1 signaling in a RAC1-dependent manner *in vivo*.

Discussion

We previously identified the HACE1 E3 ubiquitin–protein ligase as a tumor suppressor based on its loss of function in human Wilms' tumor and its ability to decrease growth in different tumor cell lines (Anglesio *et al*, 2004; Zhang *et al*, 2007). Moreover, genetic inactivation of *Hace1* in mice leads to development of multiple late-onset tumors, including sarcomas, breast, lung, and other carcinomas, and lymphomas (Zhang *et al*, 2007). A number of anti-oncogenic functions have been proposed for HACE1, including reduced expression of cyclin D1 and attenuated cell cycle progression (Zhang *et al*, 2007; Daugaard *et al*, 2013), control of autophagy through optineurin (Liu *et al*, 2014), redox regulation by inhibiting NADPH oxidases (Daugaard *et al*, 2013) or YAP functions (Zhou *et al*, 2019), reduced cell migration (Castillo-Lluva *et al*, 2013; Daugaard *et al*, 2013; Chen *et al*, 2018; El-Naggar *et al*, 2019; Zhou *et al*, 2019), altered glutamine dependency (Cetinbas *et al*, 2015), regulation of TNFR1 signaling (Tortola *et al*, 2016), and most recently, inhibition of pro-oncogenic HIF1α accumulation in tumor cells (Tortola *et al*, 2016). Several of these functions are directly linked to HACE1-mediated RAC1 degradation (Torrino *et al*, 2011; Daugaard *et al*, 2013; Turgu *et al*, 2021). However, no single mechanism explains the full spectrum of HACE1 tumor suppressor activity, suggesting that other mechanisms remain to be discovered. Here we show that HACE1 regulates stability of mTOR complexes by targeting RAC1 within the complex, revealing a ubiquitin-dependent molecular mechanism to control the activity of mTOR signaling complexes.

The mTOR protein is a component of two signaling complexes, namely mTORC1 and mTORC2. The mTORC1 complex is a central signaling node that integrates environmental cues to regulate cell survival, proliferation, metabolism, and is often deregulated in human cancers (Saxton & Sabatini, 2017). Emerging evidence supports a critical role for ubiquitin-mediated modifications as dynamically regulating the mTOR signaling pathway, although detailed mechanisms are incompletely understood (Jiang *et al*, 2019). For example, it has recently been reported that the RNF167 E3 ligase and the deubiquitinase, STAMBPL1, control polyubiquitylation levels of Sestrin2 in response to leucine availability to regulate mTORC1 activity (Wang *et al*, 2022). Moreover, TRAF6-mediated K63-linked poly-ubiquitination of RAC1 at Lys16, which promotes RAC1 activation, results in induction of both mTORC1 and mTORC2 activity (Li *et al*, 2017; Jiang *et al*, 2019). Reducing mTORC1 signaling thus provides a plausible mechanism for the anti-tumorigenic activity of HACE1, including potential roles in blocking proliferation and tumor growth. In addition to mTORC1, RAC1 has also been shown to directly associate with and regulate mTORC2 (Saci *et al*, 2011). Furthermore, active Rac1 is required for mTORC2-dependent invasion and motility (Morrison Joly *et al*, 2017). This complex controls survival, invasion and motility by phosphorylating

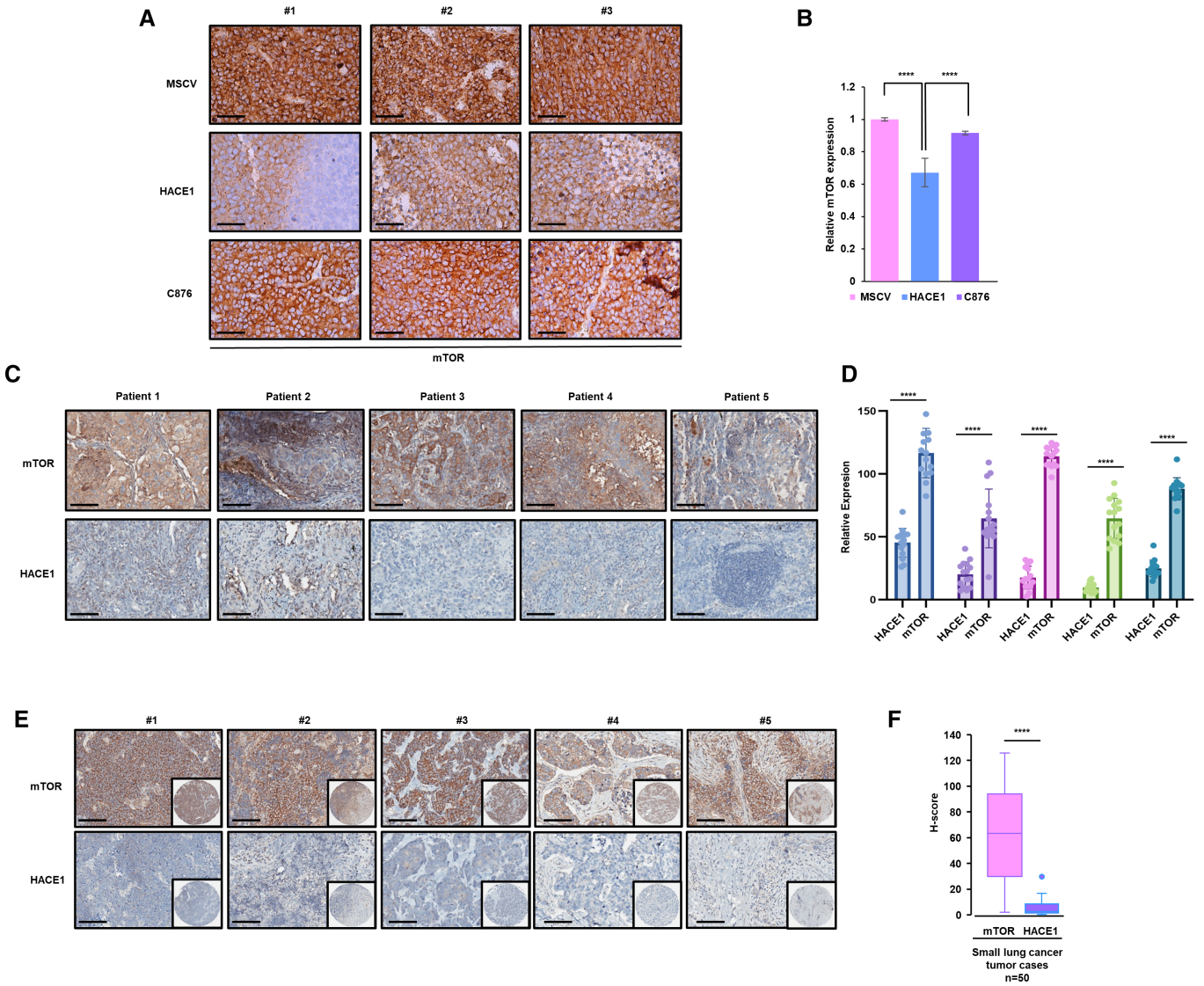

Figure 6. Loss of HACE1 expression correlates with increased mTOR expression.

A Immunohistochemistry for mTOR expression was conducted on the paraffin blocks from nude mice injected with SK-NEP-1 cells stably expressing either wild-type HACE1, HACE1-C876S, or vector alone, as previously described (3) (n = 3 mice per group, biological replicates). Scale bar is 50 μm.

B Quantification of (A) was conducted respectively using ImageJ software and data represented as average value ± SEM for n = 12 HPFs in 3 tumors/group. (n = 3 mice per group, biological replicates. paired t-test comparison test; ****$P < 0.0001$).

C Immunohistochemistry (IHC) of mTOR and HACE1 were conducted on patient samples with NSCLC (n = 5). Representative IHC images from patient samples on serial histological sections were shown (n = 3 mice per group, biological replicates). Scale bar = 50 μm.

D Quantification of (C) was conducted respectively using ImageJ software (n = 5, biological replicates). For each group 15 HPFs were analyzed. Data are shown as mean ± SEM, paired t-test comparison test (****$P < 0.0001$).

E Immunohistochemistry (IHC) of mTOR and HACE1 were conducted on serial sections of TMAs consistent with SCLC tumors (50 cases) provided by Vancouver Prostate Centre. Representative IHC images from matched patient samples on serial histological sections were shown. Scale bar = 50 μm.

F Box plot (central band: median; box limits: first and third quartile; whiskers: minimum and maximum) showing H-scores (staining intensity × percentage) for mTOR and HACE1, based on the IHC analysis in (E). (n = 50, biological replicates, paired t-test comparison test; ****$P < 0.0001$).

Source data are available online for this figure.

and activating Akt at Serine 473, which is linked to insulin/IGF1 and PI3K signaling (Saxton & Sabatini, 2017; He *et al*, 2021). We showed that HACE1 reduces p-Akt (S473) and reduces the stability of the core protein (mTOR) of both complexes (mTORC1 and mTORC2). These data argue that HACE1 also regulates mTORC2, which might explain at least in part how HACE1 reduces invasion and migration of tumor cells (El-Naggar *et al*, 2019).

We found that HACE1 reduces the stability of mTOR, suggesting that mTOR complexes may be more stable in the absence of HACE1. This was evident in both HEK293 cells with or without HACE1

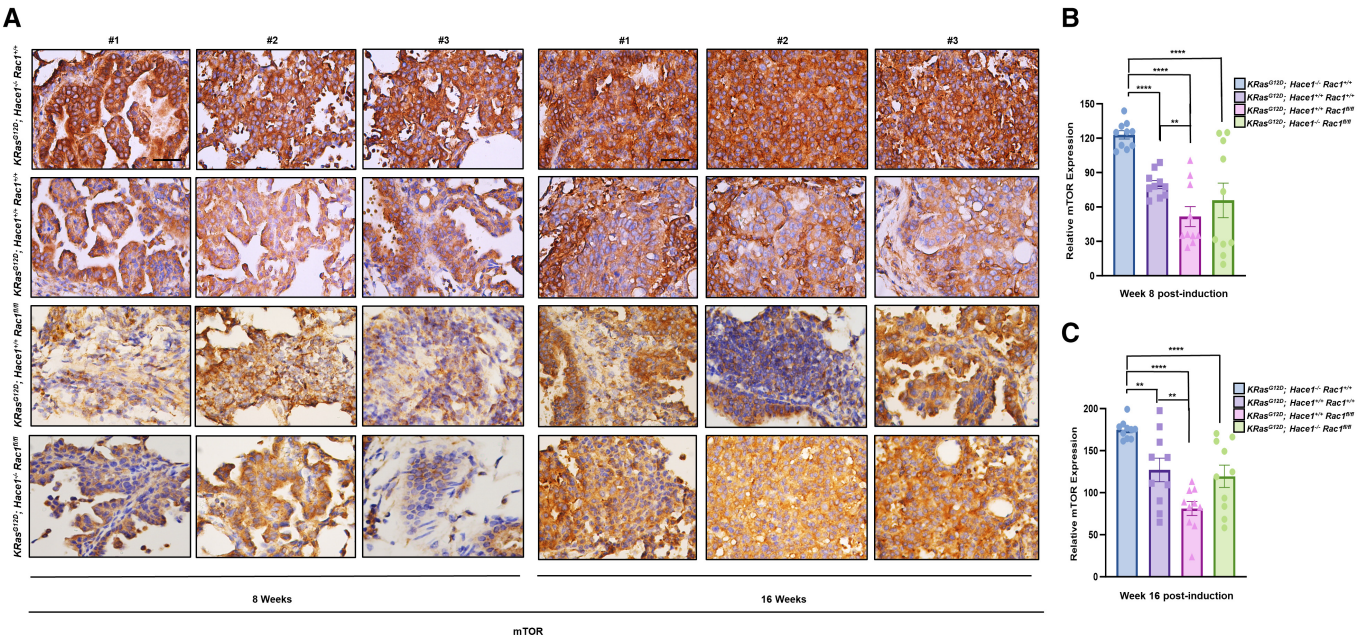

Figure 7. Genetic deletion of Rac1 reversed the increased mTOR expression of Hace1$^{-/-}$ mice.

A Immunohistochemistry for mTOR conducted on the paraffin blocks from KRasG12D-driven lung adenocarcinoma mouse model at weeks 8 and 16 after lung cancer induction for KRasG12DHace1$^{+/+}$Rac1$^{+/+}$, KRasG12DHace1$^{-/-}$Rac1$^{+/+}$, KRasG12DHace1$^{+/+}$Rac1$^{fl/fl}$, and KRasG12DHace1$^{-/-}$Rac1$^{fl/fl}$ mice, generated as described previously (34). Scale bar is 50 μm.

B Quantification of (A) (left panel) for 8 weeks after post-induction was conducted respectively using ImageJ software (n = 4 mice per group). For each group 10 HPFs were analyzed. Data are shown as mean ± SEM, paired t-test comparison test (**P < 0.01; ****P < 0.0001).

C Quantification of (A) (right panel) for 16 weeks after post-induction was conducted respectively using ImageJ software (n = 4 mice per group). For each group, 10 HPFs were analyzed. Data are shown as mean ± SEM, paired t-test comparison test (**P < 0.01; ****P < 0.0001).

Source data are available online for this figure.

over-expression, and Hace1 KO MEFs with or without HACE1 rescue. Notably, ligase dead HACE1-C876S was unable to reduce mTORC1 or mTORC2 signaling in the models tested, indicating that HACE1 E3 ligase activity is required for its effects on mTOR complexes. However, we failed to demonstrate that HACE1 directly targets mTOR for ubiquitylation and degradation. RAC1 is the best known target of the HACE1 E3 ligase (Torrino *et al*, 2011; Mettouchi & Lemichez, 2012; Castillo-Lluva *et al*, 2013; Daugaard *et al*, 2013; Goka & Lippman, 2015; Acosta *et al*, 2018), and HACE1 in part controls cell proliferation through direct ubiquitylation of RAC1, leading to its proteasomal degradation. RAC1 is a known proto-oncogene promoting tumor formation and progression (Hervieu *et al*, 2020). It has previously been shown that RAC1 regulates mTORC1 and mTORC2 activity by interacting directly with mTOR protein (Saci *et al*, 2011). In addition to RAC1, other small GTPases, including Rheb, Rag, RalA and Ryh1, also play various roles in regulating TOR activity (Xie & Proud, 2014). For example, RagC directly binds to mTORC1 depending on its active state (Saci *et al*, 2011). Moreover, RagC phosphorylation is associated with destabilization of mTORC1 (Yang *et al*, 2018), while Rheb directly binds to mTOR in its GTP bound, which is required for mTORC1 kinase activity (Saci *et al*, 2011).

Given that HACE1 decreases mTOR complex signaling in a RAC1-dependent manner, RAC1 degradation via HACE1 provides another mechanism for controlling activity of mTORC1 and mTORC2. We found that a RAC1-K147R mutant that is resistant to HACE1-mediated degradation rescued loss of mTORC1 and mTORC2 signaling in HACE1 overexpressing cells. Moreover, EHT1864, a relatively selective RAC1 activation inhibitor, almost completely mimics the effects of Rapamycin and Torin1 on blocking mTOR signaling complex activity. Consistent with these observations, stable knockdown of RAC1 in HACE1-deficient cells decreases mTORC1 and mTORC2 signaling, pointing to RAC1 targeting as a potential mechanistic intervention point for targeted therapy in diverse cancer types. We found that HACE1 physically associates with RAC1 along with mTORC1 and RAPTOR. RAC1 knockdown dramatically inhibits this interaction. While how RAC1 might interact with mTORC2 remains to be determined, our data suggest a model where HACE1 targets RAC1 once RAC1 has been recruited to mTOR signaling complexes. Furthermore, mTOR appears to be required for RAC1 ubiquitylation by HACE1, and HACE1 overexpression leads to increased levels of polyubiquitylated mTOR-associated proteins.

Most data point to FBXW7 and FBXW8 as the major E3 ligases that target mTOR for ubiquitylation and proteasomal degradation, although mainly in the context of mTORC2 complexes (Mao *et al*, 2008), while the E3 ligase for RAPTOR is unknown. It remains to be determined whether RAC1 reduction leads to enhanced mTOR degradation via FBXW8 or FBXW7. *In vivo*, loss of Hace1 markedly enhanced mTOR expression in KRasG12D-driven lung tumors. In contrast, Rac1 loss alone decreased mTOR expression in this model.

Simultaneous deletion of Hace1 and Rac1 was similar to loss of Rac1 alone and showed significantly reduced mTOR levels compared to Hace1 inactivation alone, further validating that the ability of HACE1 to reduce mTOR levels is dependent on RAC1. In non-small cell lung cancer (NSCLC) patient samples, HACE1 protein levels were virtually undetectable in all five tumor cases tested, while mTOR staining was readily detectable in each case. Verifying the potential clinical relevance of our findings in lung cancer, there was a highly significant association between strong mTOR and low to absent HACE1 expression observed in tissue microarrays of small cell lung cancer (SCLC), highlighting the inverse relationship between HACE1 and mTOR levels in these tumors, which are clinically classified as the most aggressive type of lung cancer. RAC1 and Cdc42 GTPases are key signaling intermediates with important roles in cancer initiation and progression, and inhibitors of these proteins, including EHT1864, have shown promising preclinical efficacy (Maldonado & Dharmawardhane, 2018). While none of these inhibitors have been approved for cancer therapy to date, RAC1/Cdc42 inhibition as a strategy to overcome therapy resistance has been validated previously (Rosenblatt *et al*, 2010; Gonzalez *et al*, 2017; Maldonado & Dharmawardhane, 2018), arguing for further clinical studies of these agents. Further mechanistic details of how a putative HACE1-RAC1 axis might regulate mTORC1 in the context of tumor cells, and whether other components are involved in this process, requires additional investigation.

Recently, mTOR was found to localize to focal adhesions and to be necessary and sufficient for mTORC1 activation (Rabanal-Ruiz *et al*, 2021). Focal adhesions are involved in cell polarization, spreading, and migration. Furthermore, these adhesions are required for wound healing, migration and shown to be involved in cancer cell metastasis (Byron & Frame, 2016). It was previously shown that inactivation of the total mTORC1 pool by inhibitors such as rapamycin interferes with focal adhesion dynamics and cell migration by inhibiting F-actin reorganization and phosphorylation of focal adhesion proteins (Liu *et al*, 2008). Moreover, FAK, a focal adhesion marker, reportedly has a role in the activation and translocation of RAC1 to focal adhesions (Chang *et al*, 2007). In a recent study, Optineurin, a regulator of HACE1 E3 ubiquitin ligase activity, was found to adapt FA signaling to ECM stiffness and control the number and size of FAs via regulation of RAC1 degradation through HACE1 (Petracchini *et al*, 2022). In our study, HACE1 and mTOR co-localize with FAK and Paxillin, known focal adhesion markers. One possibility is that HACE1 preferentially targets the mTORC1 complex (and potentially mTORC2) when it is activated by RAC1 within focal adhesions. This could shed light on how HACE1 limits cancer metastasis, i.e. by regulating mTORC1 and focal adhesion dynamics. It will also be of interest to determine whether modulation of mTORC1 or mTORC2 activity underlies other functions of HACE1, such as regulation of HIF1α accumulation by HACE1 in tumor cells (Turgu *et al*, 2021).

In summary, our work uncovers a previously unrecognized link between HACE1, its key E3 ligase target RAC1, and oncogenic mTOR signaling, revealing a new ubiquitin-dependent molecular mechanism to control mTOR activity. As mTOR is well established to facilitate oncogenesis in a variety of cancers, the HACE1-RAC1 axis provides an attractive potential target for therapeutic intervention.

Materials and Methods

Antibodies and reagents

For Western blot and immunofluorescence analysis, following primary antibodies were used: mTOR (7C10) Rabbit mAb (Cell Signaling Technology. Cat# 2983, RRID:AB_2105622); Phospho-mTOR (Ser2448) Antibody (Cell Signaling Technology, Cat# 2971, RRID:AB_330970); p70 S6 Kinase (49D7) Rabbit mAb (Cell Signaling Technology, Cat# 2708, RRID:AB_390722; Phospho-p70 S6 Kinase (Thr389) Antibody (Cell Signaling Technology, Cat# 9205, RRID:AB_330944); S6 Ribosomal Protein (5G10) Rabbit mAb (Cell Signaling Technology, Cat# 2217, RRID:AB_331355); Phospho-S6 Ribosomal Protein (Ser240/244) Antibody (Cell Signaling Technology, Cat #5364 RRID:AB_10694233); Phospho-S6 Ribosomal Protein (Ser235/236) Antibody (Cell Signaling Technology, Cat# 2211, RRID:AB_331679); 4E-BP1 Antibody (Cell Signaling Technology, Cat# 9452, RRID:AB_331692), Phospho-4E-BP1 (Ser65) Antibody (Cell Signaling Technology, Cat# 9451, RRID:AB_330947; Phospho-4E-BP1 (Thr37/46) (236B4) Rabbit mAb (Cell Signaling Technology, Cat# 2855, RRID:AB_560835); B-actin antibody (Cell Signaling Technology, Cat# 8457, RRID:AB_10950489); Rabbit Anti-HACE1 antibody [EPR7962] (Abcam, ab133637); Anti-HA antibody mouse mAb (Cell Signaling Technology #2367, RRID:AB_10691311); Anti-HA antibodyRabbit mAb (Cell Signaling Technology, Cat# 3724, RRID:AB_1549585); Raptor (24C12) Rabbit mAb (Cell Signaling Technology, Cat# 2280, RRID:AB_561245); mTOR (7C10) Rabbit mAb (Alexa Fluor® 647 Conjugate; Cell Signaling Technology, #5048, RRID:AB_10828101); HA Tag Monoclonal Antibody (2-2.2.14); Alexa Fluor™ 647 (Invitrogen, Cat# 26183-A647, RRID:AB_2610626); Goat anti-Rabbit IgG (H + L) Secondary Antibody, HRP (Invitrogen Cat# 31460, RRID:AB_228341); Goat anti-Mouse IgG (H + L) Secondary Antibody, HRP Invitrogen Cat# 62-6520, RRID:AB_2533947), Vinculin Cell Signaling Technology, (Cat# 13901, RRID:AB_2728768), Histone H3 (Cell Signaling Technology, Cat# 9715, RRID:AB_331563).

Cell lines

HEK293 cells were purchased from ATCC (CRL-1573) and maintained in Dulbecco's modified Eagle's medium (DMEM) containing 9% fetal bovine serum (FBS). SK-NEP-1 cells were also purchased from ATCC (HTB-48) and maintained in Dulbecco's modified Eagle's medium (DMEM) containing 9% fetal bovine serum (FBS). Authentication was conducted as stated by the provider (ATCC). Immortalized wild-type and *HACE1*$^{-/-}$ MEFs were prepared as described previously (Zhang *et al*, 2007) and cultured in DMEM containing calf serum. Cell lines stably expressing MSCV, HA-HACE1 or the mutant HA-HACE1-C876S were generated as described (Anglesio *et al*, 2004). Cells were seeded in equal number and incubated under the same conditions, then randomized and categorized into control and experimental groups in all experiments conducted unless stated otherwise.

Transfections

Transient plasmid transfections were performed using Lipofectamine 2000 (Invitrogen, #11668019) in a 6-well plate, according to

the user manual. Transfections of siRNAs were performed with 25 nM siRNA using RNAiMax (Invitrogen, # 13778075). The following siRNAs were used in the study: control siRNA (C): (5′–3′) AUAUCGGCUAGGUCUAACA; Hace1-1 (H1): Hs_Hace1_1 (FlexiTube, Qiagen, Hilden, DE); Hace1-2 (H2): Hs_Hace1_4 (FlexiTube, Qiagen); Human Rac1 (R): Hs_Rac1_6 (FlexiTube, Qiagen); and FlexiTube GeneSolution GS5879 (FlexiTube, Qiagen).

Immunohistochemistry (IHC)

IHC on tissue sections obtained from the paraffin blocks generated previously by Kogler *et al* (2020) and Zhang *et al* (2007) TMAs were constructed and provided by Vancouver Prostate Centre's Pathology Core. Unstained slides from five patient samples were provided by Dr. Wan Lam. Permission was obtained under University of British Columbia BC Cancer research ethics board certificate number H22-0369.

HACE1 and mTOR expression was assessed through IHC, which was performed using autostainers: the Ventana Discovery Ultra (for patient specimens) and Leica Bond Rx (for xenograft specimens). The following primary antibodies were prepared in SignalStain® Antibody Diluent (8112, Cell Signaling), HACE1 (1:600, ab133637, Abcam, Cambridge, UK) and mTOR (1:600 for human, 1:80 for xenograft, 2983, Cell Signaling). Anti-rabbit HRP secondary and DAB-based detection systems were used on respective platforms. Stained tissue was counterstained with hematoxylin and cover slipped. Quantitative analysis of IHC samples was conducted using ImageJ software. Pathologists were blinded to experimental hypothesis. For TMA, cores were scored for the percentages of cells positively staining for HACE1 and mTOR as well as for staining intensities using Image Scope Software with a 4-point scale (0–3+). The scoring was done automatically in a blinded manner.

GST pull-down assays

TUBEs (Tandem Ubiquitin Binding Entities) were used to purify endogenous ubiquitin conjugates from cell lysates according to the manufacturer's recommendations. Lysis buffer (20 mM Na_2HPO_4, 20 mM NaH_2PO_4, 1% NP-40, 2 mM EDTA) was supplemented with 1 mM dithiothreitol, 1 × protease inhibitor mix (Sigma) and 50 μg/ml of GST-TUBE2 (Lifesensors, Malvern, PA). One 70% confluent 10 cm dish per condition was treated as indicated, after which cells were scraped off the dish in PBS and pelleted by centrifugation. Cells were lysed in 300 μl lysis buffer and kept on ice for 20 min and lysates were cleared by centrifugation. Approximately 5% of the cleared lysates was used for input and the remaining lysate was added to 20 μl of washed Glutathione Sepharose 4 Fast flow beads (GE Healthcare) for capture of GST-TUBE2 and bound material. Reactions were kept at 4°C with rotation for 1–2 h, followed by 4 × washing in 500 μl of ice-cold TBS containing 0.1% Tween20 (TBS-T). After washing, 1× SDS Loading Buffer was added to the beads and heated at 90°C for 5–10 min and analyzed on SDS–PAGE for the indicated proteins.

Immunoblotting

Protein was extracted using NP-40 lysis buffer (50 mM Tris, pH 8.0, 150 mM NaCl, 1% NP-40, 0.5 mM EDTA, and 10% glycerol) containing protease inhibitors (Roche cOmplete™, Cat # 11697498001). 15 μg of protein was run on a 10% SDS-PAGE gel, transfered onto PVDF membranes (Millipore, Immobilon-P, Cat # IPVH20200) and blocked in 5% non-fat dry milk prepared in TBS with 0.1% Tween-20 (TBST). Three washes were performed in TBST (5 min each wash), and blots were incubated with the stated primary antibody overnight at +4°C. Next day, after three washes with TBST (5 min each wash), blots were incubated with a secondary anti-mouse or rabbit IgG-HRP antibody for 1 h at RT. All antibodies were used at a dilution of 1:1,000 unless otherwise stated. Signals were detected using Enhanced Chemiluminescence (ECL).

Immunoprecipitation

For immunoprecipitation, cells were lysed in Nonidet P-40 lysis buffer containing 100 mM NaCl, 5 mM $MgCl_2$, 2 mM EDTA, 1 mM DTT, 10 mM Tris–HCl (pH 7.6), 0.5% Nonidet P-40, 0.05% sodium deoxycholate, and 1 mM phenylmethylsulfonyl fluoride (PMSF). Cell debris was removed by centrifugation at 17,000 *g* for 20 min, and cell extracts (800 μg protein) were incubated with indicated antibodies overnight. Protein G- or A-Sepharose beads (Thermofisher, Waltham, MA, USA; 50 μl) were used to pull down antibody–protein complexes and were washed with lysis buffer for three times to remove non-specific binders. Bound proteins were eluted by boiling in 1× SDS loading buffer for 5-min. It was followed by the immunostaining protocol as described above.

Immunofluorescence microscopy and colocalization analysis

Cells were seeded in 8 well chambers previously coated with Fibronectin for 1 h at 37°C. Next day, cells were fixed with 3.7% paraformaldehyde for 12 min at RT. After the removal of paraformaldehyde, wells were washed with PBS three times. Then, cells were permeabilized with PBST for 20-min and nonspecific signaling was blocked with 4% BSA for 10-min. Each well was incubated with HA or mTOR primary antibodies directly conjugated to Alexa 647; dilution 1:100) overnight at 4°C. Next day, wells were washed with PBS with 0.05% Triton-X twice for 5 min. Chambers were carefully removed and mounted with Vectashield with DAPI (Vectorlabs). Slides were imaged using 63× objective of a Zeiss LSM 800 Airyscan confocal microscope (Carl Zeiss, Thornwood, NY). Colocalization of GFP-FAK, mcherry-Paxillin (a positive control FAK marker), and HA or mTOR (Alexa 647) were quantified using ImageJ software using JACoP Plug-in.

RAC1 G-LISA activation assay

This assay was performed according to manufacturer's detailed manual (Cytoskeleton, #BK128). 25 μg total of protein was added wells pre-coated with RAC-GTP-binding protein. Then, the plate was incubated at 4°C for 30-min followed by incubation with 50 μl of anti-RAC1 (1/50 in Antibody Dilution Buffer) for 45-min at RT. After rinsing three times with the wash buffer, the plate was incubated with a secondary antibody conjugated with HRP (1/100 in Antibody Dilution Buffer) for 45 min. Finally, 50 μl of HRP detection reagent was added to wells and

incubated for 20-min. Finally, 50 μl HRP stop solution was added to each well to stop the reaction and the absorbance was recorded at 490 nm.

RNA isolation and real time PCR

Total RNA from cells was isolated with the RNeasy Mini Kit (Qiagen). Complementary DNA (cDNA) was synthesized from total RNA with the High-Capacity cDNA Reverse Transcription Kit (Applied Biosystems). Then, quantitative PCR (qPCR) was performed using Fast SYBR™ Green Master Mix (Applied Biosystems) on QuantStudio 6 Real-Time PCR Systems (Thermo Fisher). The primers used for qPCR are as follows: 4EBP1 (forward: TCGGC GACGGCGTGCAGCT, reverse: GGTCATAGATGATCCTGGTA), S6 (forward: AGAAGTTGCTGCTGACGCT, reverse: CTTGTTTGTC GTTCCCACCA), mTOR (forward: GTCACCATGGAACTCCGAGA, reverse: GCATCTGAGCTGGAAACCAA).

Statistical analysis

Graph Pad was used to generate all graphs. SEM or STD values were calculated automatically by Graph Pad. All statistical analysis was conducted using a Student's two-tailed *T*-test, unless otherwise indicated. $P < 0.05$ considered as being statistically significant. Range of *P*-values were indicated in each experiment ($*P < 0.05$; $**P < 0.01$; $***P < 0.001$; $****P < 0.0001$).

Data availability

Images in this paper are deposited to BioStudies Archive under the S-BSST1145 accession number (https://www.ebi.ac.uk/biostudies/studies/S-BSST1145?query=S-BSST1145).

Expanded View for this article is available online.

Acknowledgements
We would like to thank Dr. Robert Nabi for providing GFP-FAK and mCherry-Paxillin plasmids. This work was supported in part by a grant to PHS from a CIHR Foundation grant (Grant#: FDN-143280) and the British Columbia Cancer Foundation through generous donations from Team Finn and other riders in the Ride to Conquer Cancer. JMP was supported by the Austrian Academy of Sciences, the T. von Zastrow Foundation, a Canada 150 Research Chairs Program (F18-01336), and CIHR grant (168899). LT was supported by the Swiss National Science Foundation (Grant#: PBEZP3_145993).

Author contributions
Busra Turgu: Conceptualization; data curation; formal analysis; validation; investigation; visualization; methodology; writing – original draft; writing – review and editing. **Amal El-Naggar:** Formal analysis; validation; investigation. **Melanie Kogler:** Resources; methodology. **Luigi Tortola:** Resources; methodology. **Hai-Feng Zhang:** Formal analysis; investigation. **Mariam Hassan:** Investigation. **Michael M Lizardo:** Formal analysis; investigation. **Sonia HY Kung:** Investigation; methodology. **Wan Lam:** Resources. **Josef M Penninger:** Resources; methodology; writing – original draft. **Poul H Sorensen:** Conceptualization; resources; supervision; funding acquisition; writing – original draft; writing – review and editing.

Disclosure and competing interests statement
Dr. Penninger is an EMBO member.

References

Acosta MI, Urbach S, Doye A, Ng Y-W, Boudeau J, Mettouchi A, Debant A, Manser E, Visvikis O, Lemichez E (2018) Group-I PAKs-mediated phosphorylation of HACE1 at serine 385 regulates its oligomerization state and Rac1 ubiquitination. *Sci Rep* 8: 1410

Anglesio MS, Evdokimova V, Melnyk N, Zhang L, Fernandez CV, Grundy PE, Leach S, Marra MA, Brooks-Wilson AR, Penninger J *et al* (2004) Differential expression of a novel ankyrin containing E3 ubiquitin-protein ligase, Hace1, in sporadic Wilms' tumor versus normal kidney. *Hum Mol Genet* 13: 2061 – 2074

Byron A, Frame MC (2016) Adhesion protein networks reveal functions proximal and distal to cell-matrix contacts. *Curr Opin Cell Biol* 39: 93 – 100

Cardama GA, Gonzalez N, Maggio J, Menna PL, Gomez DE (2017) Rho GTPases as therapeutic targets in cancer (Review). *Int J Oncol* 51: 1025 – 1034

Castillo-Lluva S, Tan CT, Daugaard M, Sorensen PH, Malliri A (2013) The tumour suppressor HACE1 controls cell migration by regulating Rac1 degradation. *Oncogene* 32: 1735 – 1742

Cetinbas N, Daugaard M, Mullen AR, Hajee S, Rotblat B, Lopez A, Li A, DeBerardinis RJ, Sorensen PH (2015) Loss of the tumor suppressor Hace1 leads to ROS-dependent glutamine addiction. *Oncogene* 34: 4005 – 4010

Chang F, Lemmon CA, Park D, Romer LH (2007) FAK potentiates Rac1 activation and localization to matrix adhesion sites: a role for betaPIX. *Mol Biol Cell* 18: 253 – 264

Chen YL, Li DP, Jiang HY, Yang Y, Xu LL, Zhang SC, Gao H (2018) Overexpression of HACE1 in gastric cancer inhibits tumor aggressiveness by impeding cell proliferation and migration. *Cancer Med* 7: 2472 – 2484

Daugaard M, Nitsch R, Razaghi B, McDonald L, Jarrar A, Torrino S, Castillo-Lluva S, Rotblat B, Li L, Malliri A *et al* (2013) Hace1 controls ROS generation of vertebrate Rac1-dependent NADPH oxidase complexes. *Nat Commun* 4: 2180

Day GJ, Mosteller RD, Broek D (1998) Distinct subclasses of small GTPases interact with guanine nucleotide exchange factors in a similar manner. *Mol Cell Biol* 18: 7444 – 7454

Duran RV, Hall MN (2012) Regulation of TOR by small GTPases. *EMBO Rep* 13: 121 – 128

El-Naggar AM, Clarkson PW, Negri GL, Turgu B, Zhang F, Anglesio MS, Sorensen PH (2019) HACE1 is a potential tumor suppressor in osteosarcoma. *Cell Death Dis* 10: 21

Fernandez CV, Lestou VS, Wildish J, Lee CL, Sorensen PH (2001) Detection of a novel t(6;15)(q21;q21) in a pediatric Wilms tumor. *Cancer Genet Cytogenet* 129: 165 – 167

Galbaugh T, Cerrito MG, Jose CC, Cutler ML (2006) EGF-induced activation of Akt results in mTOR-dependent p70S6 kinase phosphorylation and inhibition of HC11 cell lactogenic differentiation. *BMC Cell Biol* 7: 34

Gao Y, Dickerson JB, Guo F, Zheng J, Zheng Y (2004) Rational design and characterization of a Rac GTPase-specific small molecule inhibitor. *Proc Natl Acad Sci USA* 101: 7618 – 7623

Goka ET, Lippman ME (2015) Loss of the E3 ubiquitin ligase HACE1 results in enhanced Rac1 signaling contributing to breast cancer progression. *Oncogene* 34: 5395 – 5405

Gonzalez N, Cardama GA, Comin MJ, Segatori VI, Pifano M, Alonso DF, Gomez DE, Menna PL (2017) Pharmacological inhibition of Rac1-PAK1 axis

restores tamoxifen sensitivity in human resistant breast cancer cells. *Cell Signal* 30: 154 – 161

He Y, Sun MM, Zhang GG, Yang J, Chen KS, Xu WW, Li B (2021) Targeting PI3K/Akt signal transduction for cancer therapy. *Signal Transduct Target Ther* 6: 425

Hervieu A, Heuss SF, Zhang C, Barrow-McGee R, Joffre C, Ménard L, Clarke PA, Kermorgant S (2020) A PI3K- and GTPase-independent Rac1-mTOR mechanism mediates MET-driven anchorage-independent cell growth but not migration. *Sci Signal* 13: eaba8627

Hibi K, Sakata M, Sakuraba K, Shirahata A, Goto T, Mizukami H, Saito M, Ishibashi K, Kigawa G, Nemoto H *et al* (2008) Aberrant methylation of the HACE1 gene is frequently detected in advanced colorectal cancer. *Anticancer Res* 28: 1581 – 1584

Hu Y-L, Lu S, Szeto KW, Sun J, Wang Y, Lasheras JC, Chien S (2014) FAK and paxillin dynamics at focal adhesions in the protrusions of migrating cells. *Sci Rep* 4: 6024

Huang Y, de Reynies A, de Leval L, Ghazi B, Martin-Garcia N, Travert M, Bosq J, Briere J, Petit B, Thomas E *et al* (2010) Gene expression profiling identifies emerging oncogenic pathways operating in extranodal NK/T-cell lymphoma, nasal type. *Blood* 115: 1226 – 1237

Jiang Y, Su S, Zhang Y, Qian J, Liu P (2019) Control of mTOR signaling by ubiquitin. *Oncogene* 38: 3989 – 4001

Kim DH, Sarbassov DD, Ali SM, King JE, Latek RR, Erdjument-Bromage H, Tempst P, Sabatini DM (2002) mTOR interacts with raptor to form a nutrient-sensitive complex that signals to the cell growth machinery. *Cell* 110: 163 – 175

Kogler M, Tortola L, Negri GL, Leopoldi A, El-Naggar AM, Mereiter S, Gomez-Diaz C, Nitsch R, Tortora D, Kavirayani AM *et al* (2020) HACE1 prevents lung carcinogenesis via inhibition of RAC-family GTPases. *Cancer Res* 80: 3009 – 3022

Laplante M, Sabatini DM (2012) mTOR signaling in growth control and disease. *Cell* 149: 274 – 293

Li T, Qin JJ, Yang X, Ji YX, Guo F, Cheng WL, Wu X, Gong FH, Hong Y, Zhu XY *et al* (2017) The ubiquitin E3 ligase TRAF6 exacerbates ischemic stroke by ubiquitinating and activating Rac1. *J Neurosci* 37: 12123 – 12140

Liu L, Chen L, Chung J, Huang S (2008) Rapamycin inhibits F-Actin reorganization and phosphorylation of focal adhesion proteins. *Oncogene* 27: 4998 – 5010

Liu Z, Chen P, Gao H, Gu Y, Yang J, Peng H, Xu X, Wang H, Yang M, Liu X *et al* (2014) Ubiquitylation of autophagy receptor Optineurin by HACE1 activates selective autophagy for tumor suppression. *Cancer Cell* 26: 106 – 120

Maldonado MDM, Dharmawardhane S (2018) Targeting Rac and Cdc42 GTPases in cancer. *Cancer Res* 78: 3101 – 3111

Mao J-H, Kim I-J, Wu D, Climent J, Kang HC, DelRosario R, Balmain A (2008) FBXW7 targets mTOR for degradation and cooperates with PTEN in tumor suppression. *Science* 321: 1499 – 1502

Mettouchi A, Lemichez E (2012) Ubiquitylation of active Rac1 by the E3 ubiquitin-ligase HACE1. *Small GTPases* 3: 102 – 106

Morrison Joly M, Williams MM, Hicks DJ, Jones B, Sanchez V, Young CD, Sarbassov DD, Muller WJ, Brantley-Sieders D, Cook RS (2017) Two distinct mTORC2-dependent pathways converge on Rac1 to drive breast cancer metastasis. *Breast Cancer Res* 19: 74

Mossmann D, Park S, Hall MN (2018) mTOR signalling and cellular metabolism are mutual determinants in cancer. *Nat Rev Cancer* 18: 744 – 757

Murugan AK (2019) mTOR: role in cancer, metastasis and drug resistance. *Semin Cancer Biol* 59: 92 – 111

Onesto C, Shutes A, Picard V, Schweighoffer F, Der CJ (2008) Characterization of EHT 1864, a novel small molecule inhibitor of Rac family small GTPases. *Methods Enzymol* 439: 111 – 129

Petracchini S, Hamaoui D, Doye A, Asnacios A, Fage F, Vitiello E, Balland M, Janel S, Lafont F, Gupta M *et al* (2022) Optineurin links Hace1-dependent Rac ubiquitylation to integrin-mediated mechanotransduction to control bacterial invasion and cell division. *Nat Commun* 13: 6059

Rabanal-Ruiz Y, Byron A, Wirth A, Madsen R, Sedlackova L, Hewitt G, Nelson G, Stingele J, Wills JC, Zhang T *et al* (2021) mTORC1 activity is supported by spatial association with focal adhesions. *J Cell Biol* 220: e202004010

Rosenblatt AE, Garcia MI, Lyons L, Xie Y, Maiorino C, Desire L, Slingerland J, Burnstein KL (2010) Inhibition of the Rho GTPase, Rac1, decreases estrogen receptor levels and is a novel therapeutic strategy in breast cancer. *Endocr Relat Cancer* 18: 207 – 219

Saci A, Cantley LC, Carpenter CL (2011) Rac1 regulates the activity of mTORC1 and mTORC2 and controls cellular size. *Mol Cell* 42: 50 – 61

Sakata M, Kitamura YH, Sakuraba K, Goto T, Mizukami H, Saito M, Ishibashi K, Kigawa G, Nemoto H, Sanada Y *et al* (2009) Methylation of HACE1 in gastric carcinoma. *Anticancer Res* 29: 2231 – 2233

Saxton RA, Sabatini DM (2017) mTOR signaling in growth, metabolism, and disease. *Cell* 168: 960 – 976

Shutes A, Onesto C, Picard V, Leblond B, Schweighoffer F, Der CJ (2007) Specificity and mechanism of action of EHT 1864, a novel small molecule inhibitor of Rac family small GTPases. *J Biol Chem* 282: 35666 – 35678

Slade I, Stephens P, Douglas J, Barker K, Stebbings L, Abbaszadeh F, Pritchard-Jones K, Cole R, Pizer B, Stiller C *et al* (2010) Constitutional translocation breakpoint mapping by genome-wide paired-end sequencing identifies HACE1 as a putative Wilms tumour susceptibility gene. *J Med Genet* 47: 342 – 347

Stewenius Y, Jin Y, Ora I, Panagopoulos I, Moller E, Mertens F, Sandstedt B, Alumets J, Akerman M, Merks JH *et al* (2008) High-resolution molecular cytogenetic analysis of Wilms tumors highlights diagnostic difficulties among small round cell kidney tumors. *Genes Chromosomes Cancer* 47: 845 – 852

Thelander EF, Ichimura K, Corcoran M, Barbany G, Nordgren A, Heyman M, Berglund M, Mungall A, Rosenquist R, Collins VP *et al* (2008) Characterization of 6q deletions in mature B cell lymphomas and childhood acute lymphoblastic leukemia. *Leuk Lymphoma* 49: 477 – 487

Torrino S, Visvikis O, Doye A, Boyer L, Stefani C, Munro P, Bertoglio J, Gacon G, Mettouchi A, Lemichez E (2011) The E3 ubiquitin-ligase HACE1 catalyzes the ubiquitylation of active Rac1. *Dev Cell* 21: 959 – 965

Tortola L, Nitsch R, Bertrand MJM, Kogler M, Redouane Y, Kozieradzki I, Uribesalgo I, Fennell LM, Daugaard M, Klug H *et al* (2016) The tumor suppressor hace1 is a critical regulator of TNFR1-mediated cell fate. *Cell Rep* 15: 1481 – 1492

Turgu B, Zhang F, El-Naggar A, Negri GL, Kogler M, Tortola L, Johnson F, Ng T, Li A, Yapp D *et al* (2021) HACE1 blocks HIF1α accumulation under hypoxia in a RAC1 dependent manner. *Oncogene* 40: 1988 – 2001

Wang D, Xu C, Yang W, Chen J, Ou Y, Guan Y, Guan J, Liu Y (2022) E3 ligase RNF167 and deubiquitinase STAMBPL1 modulate mTOR and cancer progression. *Mol Cell* 82: 770 – 784

Xie J, Proud CG (2014) Signaling crosstalk between the mTOR complexes. *Translation (Austin)* 2: e28174

Yang G, Humphrey SJ, Murashige DS, Francis D, Wang Q, Cooke KC, Neely GG, James DE (2018) RagC phosphorylation autoregulates mTOR complex 1. *EMBO J* 38(3): 1 – 2

Zhang L, Anglesio MS, O'Sullivan M, Zhang F, Yang G, Sarao R, Mai PN, Cronin S, Hara H, Melnyk N *et al* (2007) The E3 ligase HACE1 is a critical chromosome 6q21 tumor suppressor involved in multiple cancers. *Nat Med* 13: 1060 – 1069

Zhou Z, Zhang HS, Zhang ZG, Sun HL, Liu HY, Gou XM, Yu XY, Huang YH (2019) Loss of HACE1 promotes colorectal cancer cell migration via upregulation of YAP1. *J Cell Physiol* 234: 9663 – 9672